JOURNAL OF GEOPHYSICAL RESEARCH, VOL. 104, NO. B9, PAGES 20,221–20,235, SEPTEMBER 10, 1999

Regional waveform propagation in the Arabian Peninsula

Robert J. Mellors and Victor E. Camp

Department of Geological Sciences, San Diego State University, San Diego, California

Frank L. Vernon

Cecil and Ida Green Institute of Geophysics and Planetary Physics, Scripps Institute of Oceanography, La Jolla, California

Abdullah M. S. Al-Amri and Ali Ghalib

Department of Geology, King Saud University, Riyadh, Kingdom of Saudi Arabia

Abstract. Regional waveform propagation is characterized in the Arabian Peninsula using data from a temporary network of broadband seismometers. Between November 1995 and March 1997, 332 regional (delta $< 15°$) events were recorded from nine stations deployed across the Arabian Shield. Regional phase propagation was analyzed in two ways: by individual inspection of the waveforms and by stacking of waveforms. Inspection of the waveforms revealed consistent variations in individual seismograms according to the region of origin. Waveforms from events in the Gulf of Aqaba, northwest of the network, possess weak *Pn*, *Pg*, and *Sn* but show a prominent *Lg* phase. In contrast, clear *Pn*, *Sn*, and *Lg* are observed for events located in the Zagros, a region northeast of the network. Events near the Straits of Hormuz also display *Pn* and *Sn* but lack a strong high-frequency *Lg*. Southern Red Sea and African earthquakes have moderate-amplitude body phases with some *Lg*. For the stacks the data were high-pass filtered at 1 Hz, rectified, binned, and then stacked by time/distance or by time/slowness. The time/distance stacks show clear differences between regions that correspond to the variations observed in individual seismograms. The time/slowness stacks allow comparison of relative phase velocities and amplitudes. *Pn* velocity under the network was estimated to be 8.0 ± 0.2 km/s, consistent with data from prior refraction profiles. The area of inefficient *Pn* and *Sn* propagation coincides with an area of Holocene volcanism and suggests that anomalous upper mantle underlies much of the Arabian Shield.

1. Introduction

Variations in the propagation of regional phases have long been used in regional tectonic studies [e.g., *Molnar and Oliver*, 1969; *McNamara et al.*, 1995]. Recently, regional phase studies have also played an important role in Comprehensive Test Ban Treaty research [*Dowla et al.*, 1996]. In this paper we analyze the propagation of *Pn*, *Sn*, and *Lg* in the Arabian Peninsula. We find that that significant differences exist in regional phase propagation throughout the Arabian Peninsula and that stacking is an effective method of characterizing regional wave propagation. In particular, inefficient *Sn* propagation across much of western Saudi Arabia may be due to an anomalous mantle that extends well east of the Red Sea rifting.

Paper number 1999JB900187.
0148-0227/99/1999JB900187$09.00

Although considerable work has been done on regional wave propagation in the Middle East [*Kadinsky-Cade et al.*, 1981; *McNamara et al.*, 1996b; *Rodgers et al.*, 1997; *Dowla et al.*, 1996], detailed analysis of propagation within the Arabian Peninsula has been hampered by a lack of stations in Saudi Arabia. As most available data consisted of signals that transverse the entire peninsula, it was difficult to isolate specific areas of blockage or attenuation. The data presented here are the first widely available broadband waveform data from the interior of the Arabian Peninsula.

The Arabian Peninsula comprises much of the Arabian plate, a subplate split from the African plate by rifting along the Red Sea (Figure 1). Active rifting also occurs along the southern edge of the Arabian plate in the Arabian Sea. As the Arabian plate moves north-

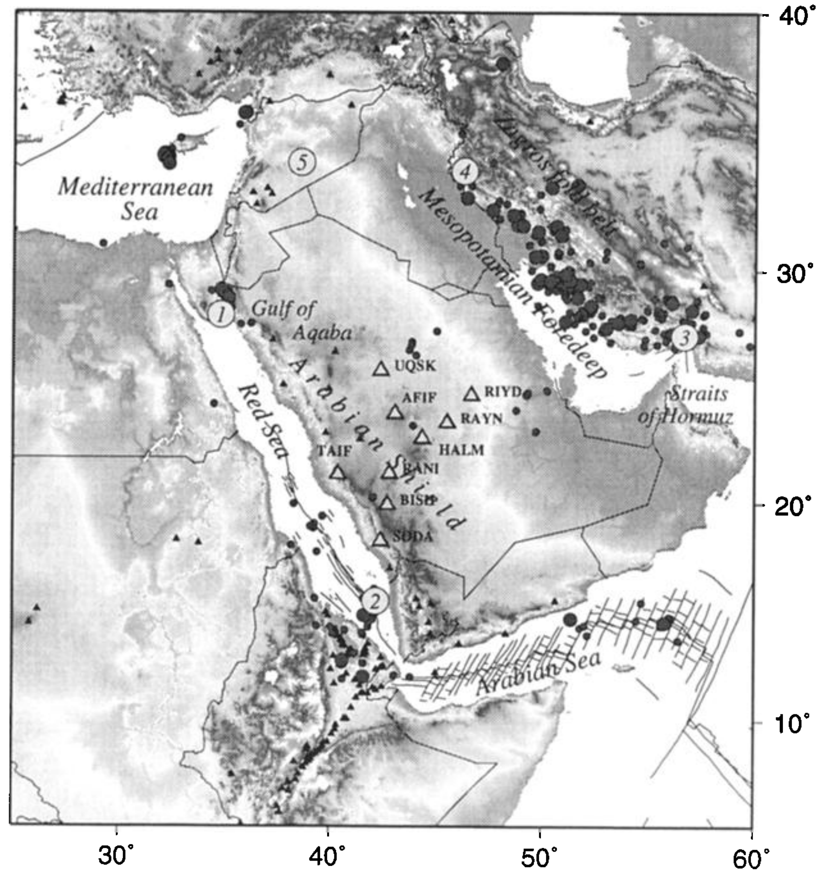

Figure 1. Elevation map of the Arabian Peninsula. Open triangles mark station locations. Small solid triangles denote Holocene volcanic activity (Smithsonian Institution, Global Volcanism Program, 1997, data available at http://www.volcano.si.edu/gvp). Small circles denote earthquakes with $m_b < 4.5$ and larger circles are earthquakes with $m_b > 4.5$ recorded by this network. Numbered circles mark the locations of events shown in Figure 2. Magnetic lineations and fracture zones are also shown (National Oceanic and Atmospheric Administration, 1998, data available at http://www.aist.go.jp). All figures created using Generic Mapping Tools software [Wessel and Smith, 1995].

ward away from the rifting, it collides with the Eurasian plate to the northeast, creating the seismically active Zagros fold-and-thrust belt [*Barazangi et al.*, 1993].

Geologically, the Arabian Peninsula is split into two main regions: Precambrian shield in the west and a stable platform of Phanerozoic sedimentary rocks in the east. The platform sediments dip and thicken greatly into the Mesopotamian Foredeep [*Seber et al.*, 1997; *Ross et al.*, 1986] along the northeast boundary of the plate. The Arabian Shield is composed of at least five geologically distinct accreted terranes separated by four ophiolite-bearing suture zones [*Stoeser and Camp*, 1985]. Unlike a typical shield, the Arabian Shield contains areas of volcanism, especially in the western section [*Camp et al.*, 1987, 1991; *Camp and Roobol*, 1992] (Figure 1).

Previous studies of the Arabian Shield based on a 1978 refraction line [*Healy et al.*, 1982; *Gettings et al.*, 1986; *Mooney et al.*, 1985; *Mechie et al.*, 1986] indicate a crustal thickness of 40 km and a velocity structure similar to other shield regions. A receiver function study [*Sandvol et al.*, 1998] using the same data presented in this paper also found crustal thickness of 35 to 40 km. Regional surface wave studies by *Ghalib* [1992] suggest that crustal and upper mantle velocities are high, although *Knox et al.* [1998] found low mantle velocities under selected paths in western Saudi Arabia. However, attenuation in the region appears to be high [*Mitchell and Pan*, 1996; *Seber and Mitchell*, 1992]. Evidence from xenoliths [*McGuire*, 1988] suggests higher than average lithospheric temperatures under western Arabia.

Prior studies of regional phases indicate *Pn* velocities > 8.0 km/s for most of the peninsula with slower values along the Red Sea [*Rodgers et al.*, 1997; *Hearn and Ni*, 1994]. *Lg* propagates in the northern section of the peninsula, as does *Sn* with the exception of the Gulf of Aqaba region. *Lg* is partially blocked in the Zagros and entirely blocked in the Red Sea [*Rodgers et al.,* 1997].

2. Method and Results

2.1. Overview of Data Set

The data analyzed in this study were recorded at nine stations installed across the Saudi Arabian shield region from November 1995 to March 1997. The deployment was a collaborative effort by the University of California, San Diego (UCSD), King Saud University (KSU), King Abdul-Aziz City of Science and Technology (KACST), and Boise State University. Data were recorded continuously at 40 samples/s using broadband Steckeisen STS-2 seismometers in combination with 24-bit Reftek data loggers [*Vernon et al.,* 1996]. The stations were located on bedrock sites, and most had low noise levels [*Mellors,* 1997]. Eight stations were located on the Arabian Shield. One station (RIYD) was situated on the Arabian Platform. Not all stations were operational during the entire experiment due to instrument relocations and equipment problems. The Arabian Shield itself is seismically quiet, but the seismically active regions at the boundaries of the Arabian plate provide regional sources in almost all directions [*Al-Amri,* 1990, 1994, 1995].

Initially, all data were passed through an automatic phase picker. The phase arrivals were reviewed manually and compared with expected arrivals using the Reviewed Event Bulletin (REB) catalog (International Data Center, 1998, data available at http://inge.css.gov). If the event was not in the REB, we determined our own location using a regional location program based on the International Association of Seismology and Physics of the Earth's Interior (IASPEI) travel time tables [*Kennett and Engdahl,* 1991].

Most of the recorded local/regional events occurred at the boundaries of the Arabian Peninsula, and only 12 events were located within the peninsula at distances $< 5°$from the nearest station. All of these local events were small. We suspect (based on time of origin) that at least four events are likely quarry blasts, but the identity of the other events is uncertain. We do not have a comprehensive list of all quarries or mines in the region, so it is difficult to precisely identify the events.

A majority of the regional events occurred to the east of the network in the Zagros. A cluster of aftershocks from the November 22, 1995, Gulf of Aqaba M_w 7.1 event was also recorded, along with activity in the Arabian Sea and southern Red Sea. There were also a few events in the eastern Mediterranean. While reviewing the data and locations, we noticed striking and consistent differences in the waveforms according to region of origin (Figures 2a and 2b). These differences were noted by F. Ryall (1997, data available at http://www.multimax.com/gtdb, herein referred to as unpublished) as well, who also conducted a careful waveform-by-waveform analysis of the Saudi data set.

Events from the Gulf of Aqaba region (event 1 on Figure 2a) show a pronounced *Lg* wave. *Pn*, *Pg*, and *Sn* were weak and emergent even for events larger than m_b 4.0. F. Ryall (unpublished, 1997) picked *Sn* and *Pg* on $\sim$ 10% of the waveforms from the Gulf of Aqaba and only at stations RAYN and HALM. Waveforms from the event shown in Figure 2b appear very similar to the Gulf of Aqaba events with a strong *Lg* but with slightly more pronounced *Sn*. RIYD, the easternmost station, had both a clear *Sn* and *Pg*.

In contrast, data from the northeast (Zagros region) have clear *Pn*, *Sn*, and *Lg* on most waveforms, with *Pg* visible at closer distances (event 4 on Figure 2a). However, data from the Straits of Hormuz region (event 3 on Figure 2a) lack a clear high-frequency *Lg* but show an impulsive *Sn*. The F. Ryall (unpublished, 1997) study also noted a "slow" *Lg* phase.

Red Sea events (event 2 on Figure 2a) have *Lg* but also show observable *Pn* and *Sn*. Finally, events from the Arabian Sea, which travel partly through oceanic crust, are lower frequency with pronounced dispersion of surface waves.

We conducted a systematic qualitative study of the variations in *Sn* and *Lg* using the method of *Rodgers et al.* [1997]. Waveforms from events larger than m_b 4.0 were filtered (three pole zero-phase Butterworth between 0.5 and 5.0 Hz), windowed according to specified velocities (between 4.1 and 4.6 km/s for *Sn* and 3.0 and 3.6 km/s for *Lg*), and manually examined. *Sn* and *Lg* phases were classified as efficient (onset of phase easily identifiable), inefficient (onset less clear), or unobserved (onset very difficult to see). The signal-to-noise ratio was poor for many smaller events, and we show only results for larger events ($m_b > 4.3$) (Figure 3). Efficient *Sn* is observed for events to the northeast. *Sn* in the Gulf of Aqaba region is not observed or inefficient, but *Lg* is efficient. *Lg* is weak for events near the Straits of Hormuz.

A difficulty with this method is that it is subjective. While the overall qualitative results may be similar, it is unlikely that different analysts will pick all events exactly the same, especially for emergent phases. Another approach is to compute ratios between phase amplitudes (*Sn*/*Pn* or *Lg*/*Pn*) [e.g., *Rodgers et al.*, 1997; *Hartse et al.*, 1998]. *Rodgers et al.* [1997] noted that this worked well for characterizing *Lg* propagation but not so well for *Sn*. We tested this approach and also found a large scatter for *Sn*/*Pn*. Part of the scatter is because both *Pn* and *Sn* for Gulf of Aqaba events are very low amplitude and barely above background noise for even the largest events. We also found a wide variation in *Lg* velocities with azimuth that required inspection of the waveforms to ensure the windows enclosed the peak amplitudes.

For these reasons, we decided to test an alternate approach: to stack the data. This possesses several po-

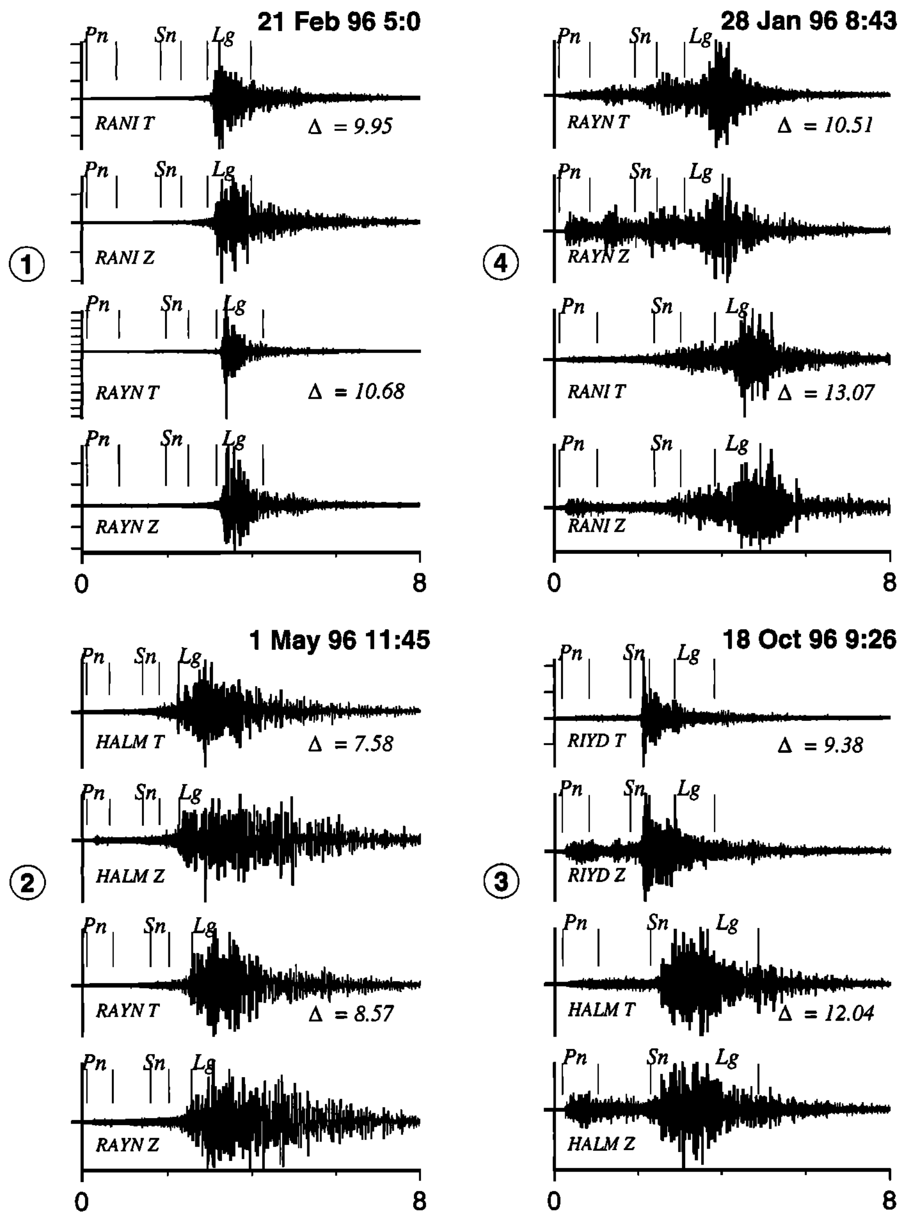

Figure 2a. Representative waveforms (vertical and transverse components) for events 1 through 4 shown in Figure 1. Seismograms have been band-pass filtered from 0.5 to 5 Hz. Vertical lines show the windows used for phase identification (*Pn* 6.2 to 8.1 km/s; *Sn* 4.1 to 4.6 km/s; and *Lg* 3.0 to 3.6 km/s). Event 1 (Gulf of Aqaba) has strong *Lg* but weak *Sn*. In comparison, event 3 (Straits of Hormuz) has strong *Sn* but weak *Lg*.

tential advantages over previous methods. All data are used, even small-amplitude events, which would be difficult to analyze using single-seismogram methods. The stacks reflect the average signal, minimizing any problems caused by individual abnormal waveforms from source effects (such as multiple ruptures, unusual depth, or directivity). The data can be processed quickly, and the results are easily presentable and understandable.

Previously, waveform stacking has been used to image global waveforms [*Shearer,* 1991, 1994; *Astiz et al.,* 1996] as well as to resolve crustal [*Richards-Dinger and Shearer,* 1997] and mantle structure [*Walck and Clayton*, 1984; *Vidale and Benz*, 1992; *Flanagan and Shearer*, 1998; and *Earle and Shearer*, 1998].

2.2. Stack Processing

The data were subset to include only ray paths between 5°and 15°. These cutoffs were chosen to ensure that the first *P* arrival was *Pn*, rather than *Pg* at short distances or direct *P* (i.e., mantle triplication phases) at longer distances.

The stacking follows a modified version of the procedures used in earlier studies [*Shearer* 1991, 1994; *Astiz et al.*, 1996; *Earle and Shearer*, 1998; and *Richards-*

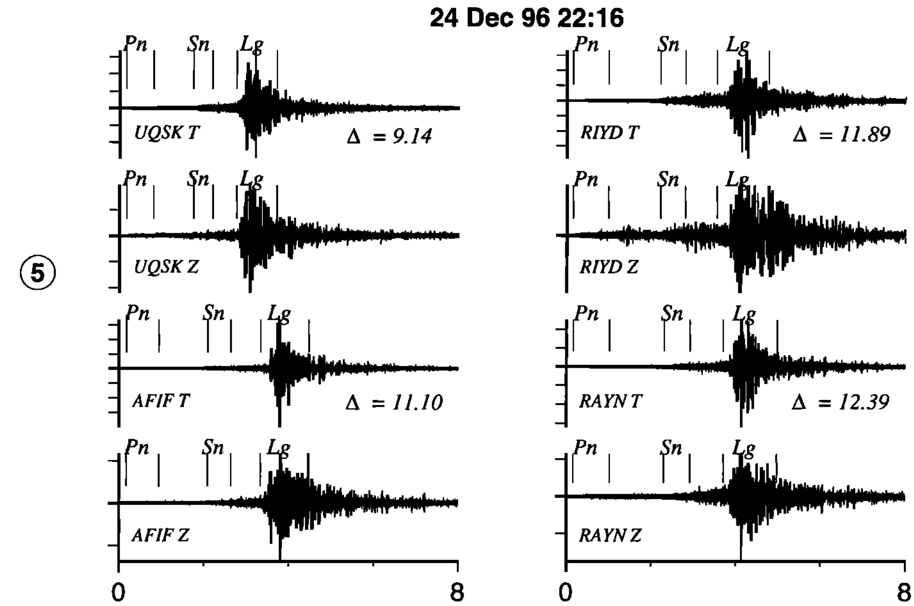

Figure 2b. Vertical and transverse seismograms for a m_b 4.3 event (event 5 on Figure 1). Using the classification scheme in this paper, *Sn* was "inefficient" at RIYD, RAYN, and UQSK and "not observed" at AFIF. *Lg* was "efficient" at all four stations.

Dinger and Shearer, 1997]. The waveforms are extracted from the continuously recorded 40 samples/s data, demeaned, and then filtered. We applied a 1-Hz high pass (three-pole zero phase Butterworth). The absolute value was taken, and the data were averaged by time into 1-s blocks (binned) using the *P* arrival time as a reference. Each trace was normalized using the peak bin amplitude per trace. The traces were then grouped by the calculated station-to-event distance. All traces with the same distance were stacked together. We used a distance bin size of 0.25°, so, for example, all traces between 7.00°and 7.25°were stacked. Because the binning is dependent only on the event-station distance and the *P* arrival time, small errors in epicentral location do not greatly affect the stacks. We also calculated various simple statistics such as the minimum, maximum, range, and standard deviation for all the bins.

2.3. Amplitude Stacks

On the basis of the previously noted geographic distribution of waveforms, we divided the data into groups. These groups (see Figure 3) were based largely on the pattern of recorded seismicity and correspond to the clusters of seismicity present in Figure 1: Zagros events (NE, 169 events), Gulf of Aqaba (NW, 25 events), and the Red Sea (SW, 39 events).

Clear differences in the waveform stacks (Figure 4) are immediately apparent. A strong high-frequency phase with a velocity of about 3.5 km/s is visible on both vertical and transverse component stacks of Gulf of Aqaba events (NW). We interpret this phase as *Lg*. *Pn*, *Sn*, and *Pg* are not visible on these stacks, indicating that the arrivals are very small compared to the surface waves. Stacks of Zagros events (NE), in contrast, have clear body waves. In addition to *Pn* and *Sn* the stacks show a later phase, presumably *Lg*, but slower than 3.5 km/s.

The stacks of southern Red Sea and African events (SW) are not as clear, and the move-out is not as well defined, probably due to a variety of complex paths through both oceanic and continental crust as well as a smaller amount of data. *Pn* and *Sn* arrivals are present, along with *Lg*.

The large amount of data from the northeast (Zagros) allows a further subdivision of the data (Figure 5). We separated the events into three groups: NE1 (near the Straits of Hormuz), NE2 (northeast of the Arabian Gulf), and NE3 (near the Iran/Iraq border) (see also Figure 3). The Straits of Hormuz (NE1) stacks show pronounced *Sn* and *Pn* but a weak *Lg*. In comparison, a clear *Lg* phase is present (between 3.0 and 3.5 km/s) on the NE2 and NE3 stacks. The NE2 and NE3 stacks also indicate *Pn* and *Sn* (and *Pg* for the nearer events).

2.4. Phase Detection Stacks

A drawback of the amplitude stacks is that the largest phases are emphasized over the weaker phases due to the trace normalization. This feature is particularly noticeable in the Gulf of Aqaba stacks, in which the weak *Pn* arrival is not visible. One solution is to use a detection filter which emphasizes phase arrivals rather than maximum amplitudes [*Astiz et al.*, 1996]. For this study we used a detection filter based on a moving average ratio calculated between two equal-length windows before and after each sample. We used 1-s windows applied to the 1.0-Hz high-pass-filtered data. The sen-

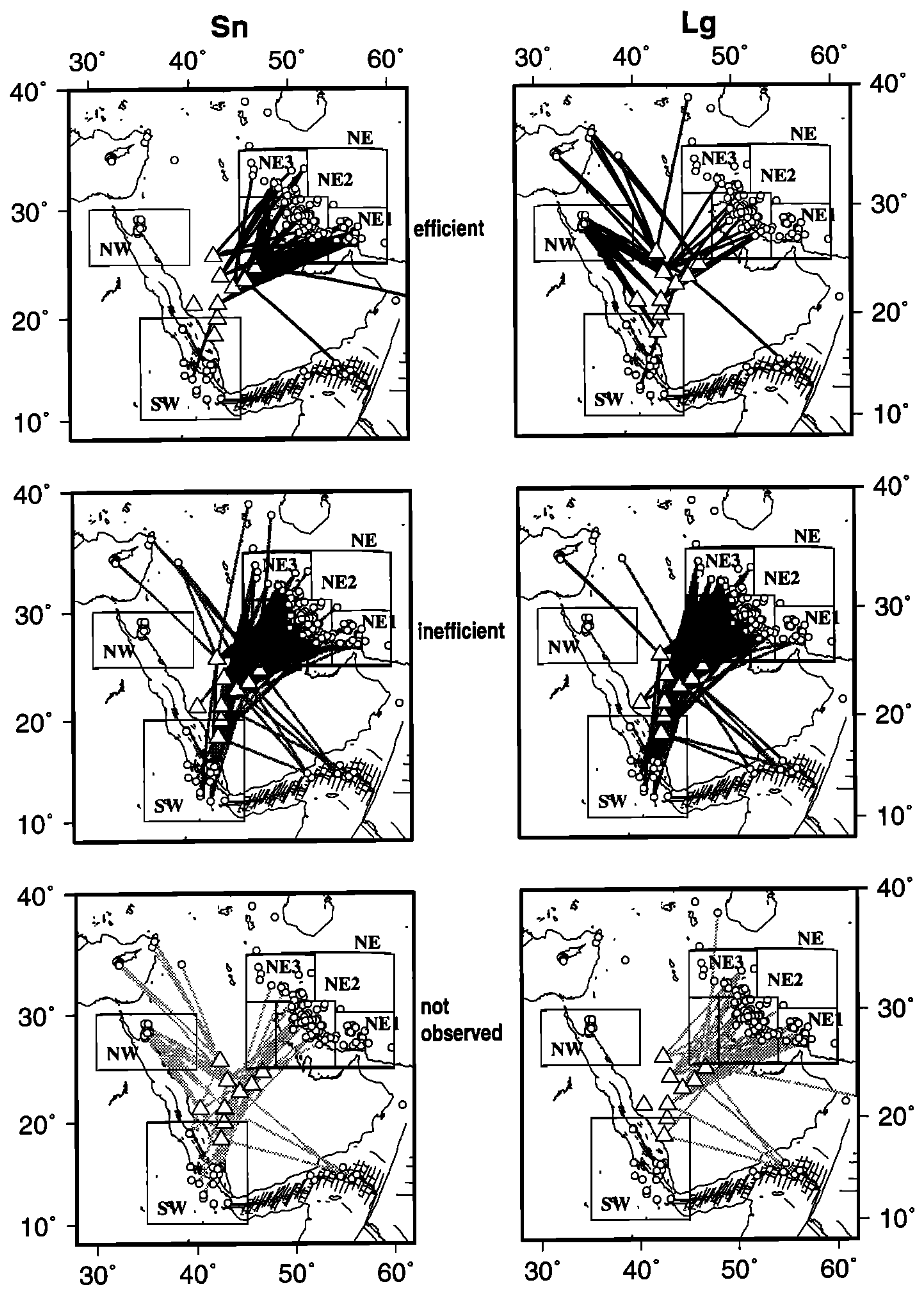

Figure 3. Propagation characteristics of *Sn* and *Lg* as determined by inspection of seismograms of events with $m_b > 4.3$. The larger boxes (NE, NW, and SW) outline clusters of events used in Figure 4. The smaller boxes (NE1, NE2, and NE3) show subsets of events used in stacks shown in Figure 5.

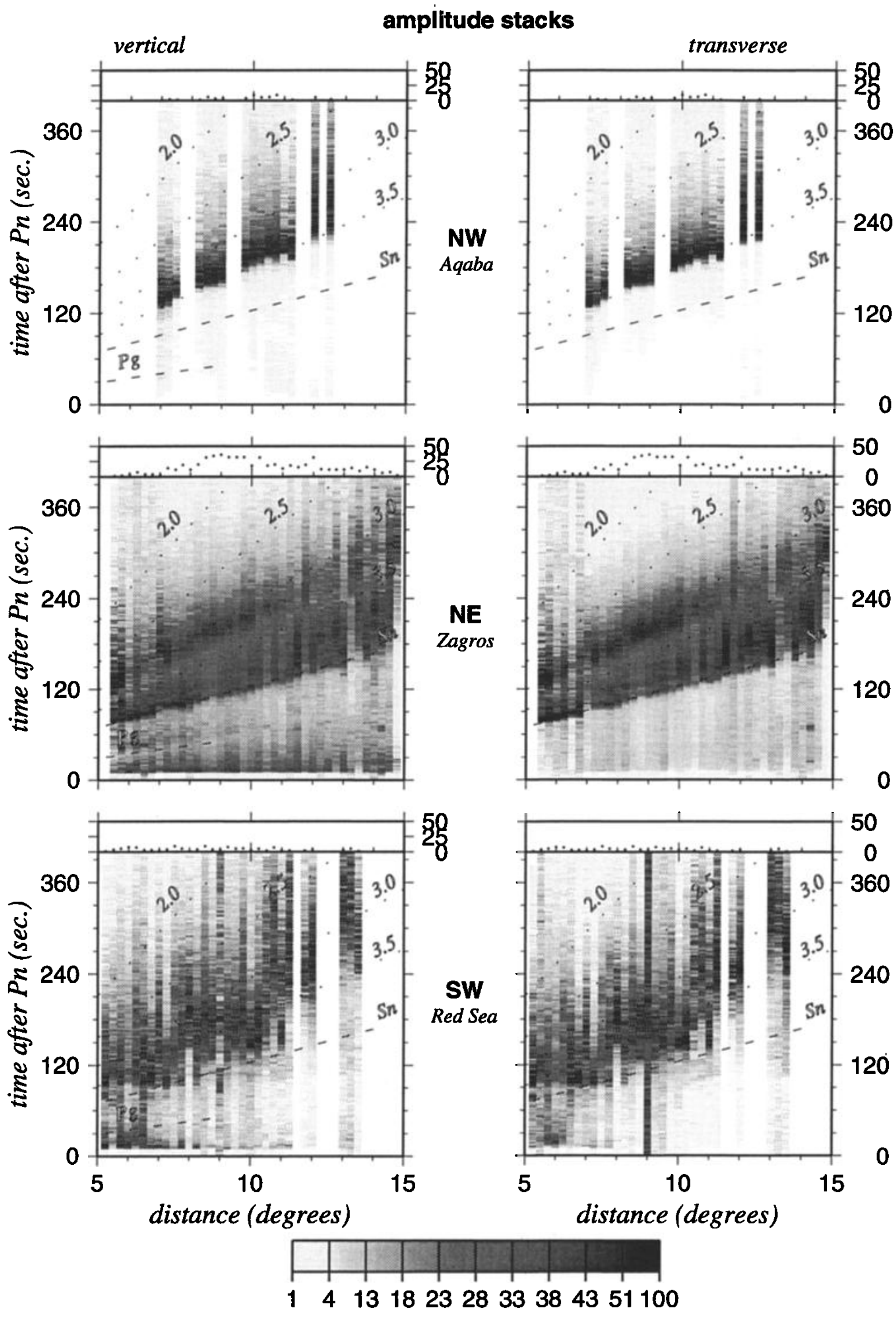

Figure 4. High-frequency stacks (vertical and transverse components) of waveforms grouped by location. The NW stack consists of events from the Gulf of Aqaba region. The NE stack includes events from across the Arabian Gulf in the Zagros Mountains and the SW stack is of events in the southern Red Sea and Africa. Dashed lines indicate phase arrival times based on the IASPEI travel time tables for *Pg* and *Sn*, and dotted lines indicate surface waves traveling at 3.5, 3.0, 2.5, and 2.0 km/s.

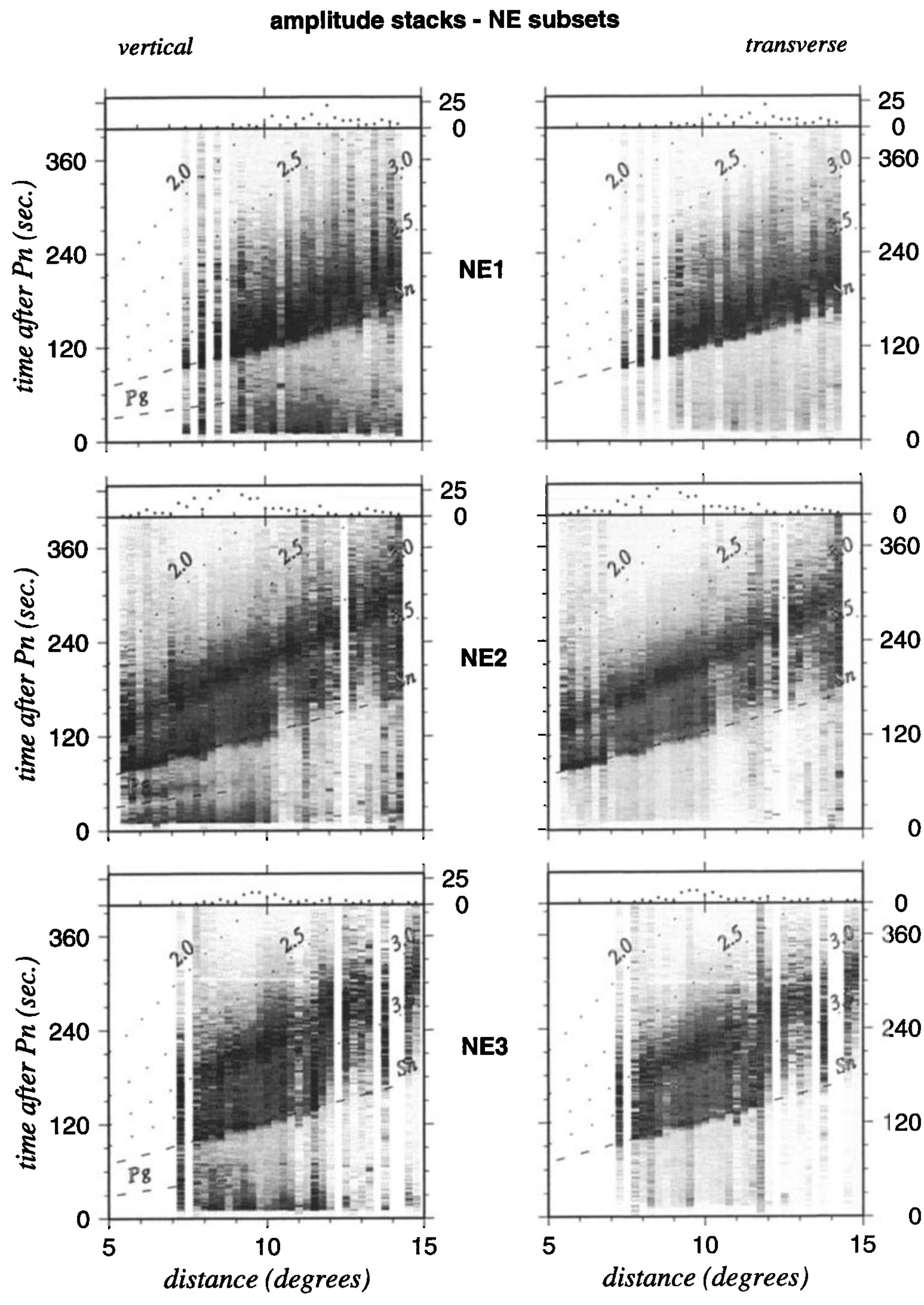

Figure 5. High-frequency stacks of waveforms for the vertical and transverse components for three clusters of earthquakes northeast of the network (see Figure 3). Note the strong impulsive *Sn* for waveforms and weak *Lg* from region NE1 as compared to the other regions. Scale is same as in Figure 4.

sitivity of the detection depends on both the window length and the characteristics of the arrival. To avoid large ratios caused by impulsive arrivals, a maximum value of 7 was set.

This is a noncausal filter, but for an impulsive arrival, the filtered peak amplitude will coincide with the non-filtered first-break arrival time. For emergent arrivals the filtered peak amplitude may be delayed relative to the first visible arrival on the non-filtered data. This is a difficult problem, as regional phases frequently display emergent arrivals. We note that is a problem even with first-break picking, as the onset time of emergent arrivals depends greatly on the background noise level.

Figure 6 shows the detection stacks calculated relative to the *Pn* arrival time as before. The filter easily detects the first *Pn* as well as the *Lg* for the Gulf of Aqaba data. However, no *Sn* arrival is detected. The stacks of data from earthquakes to the northeast show clear *Pn*, *Pg*, *Sn*, and *Lg* arrivals. Interestingly, a possible faint arrival is also present a few seconds after *Sn* in the 8°-10°range. Unfortunately, this filter does not work well with the data from the Red Sea region, probably due to slightly lower frequencies and fewer data. Figure 6 (bottom) compares the results of the detection filter (contoured by amplitude) with phase picks (crosses) made manually on the same data set. The two results correspond, indicating that the detection filter does not introduce a large delay or a systematic bias.

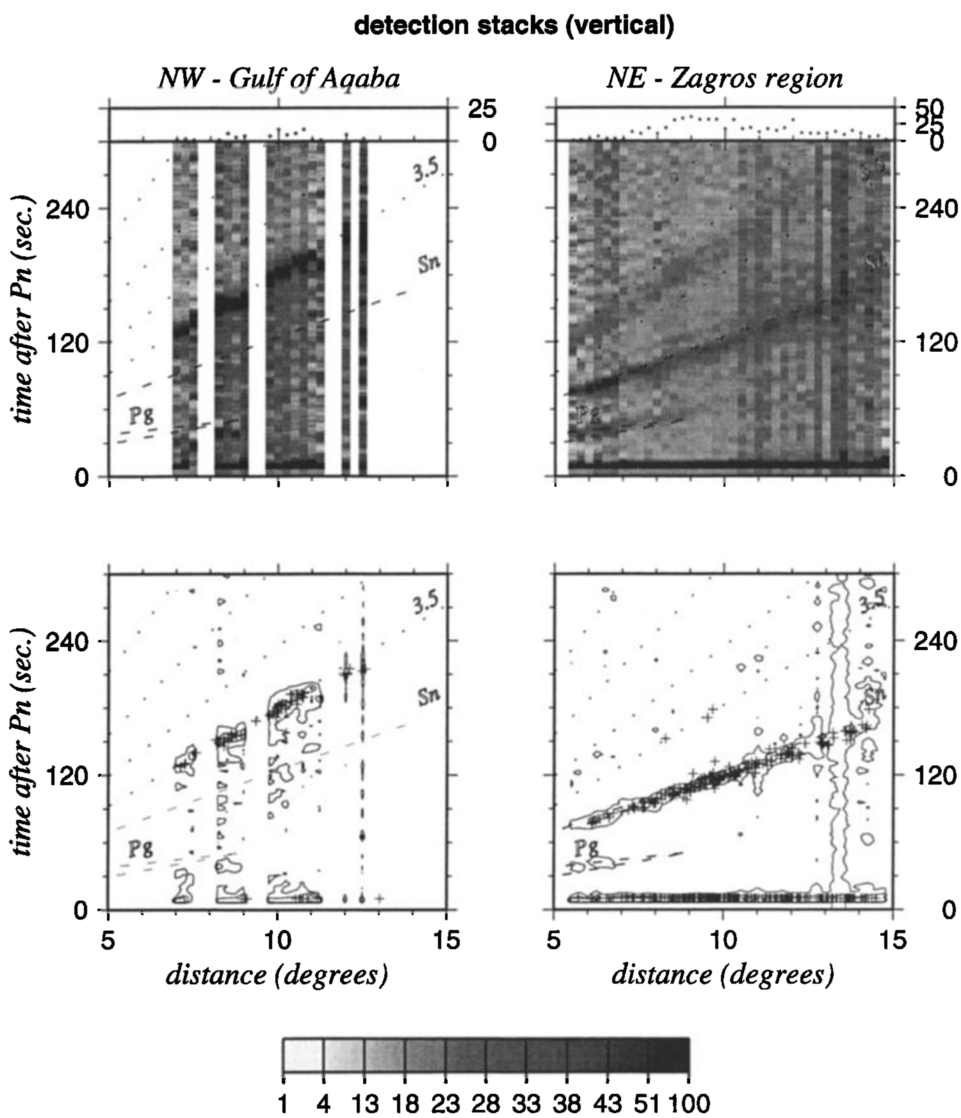

Figure 6. (top) Phase detection stacks for the Gulf of Aqaba and for events to the northeast. *Pn* is detected for Gulf of Aqaba events and *Pg* is detected for northeastern events. A secondary phase may be present just after *Sn* in the 8°-10°range for events from the northeast. (bottom) Comparison of contoured phase detection stacks with manually picked phases (small crosses).

2.5. Regional Phase Velocities

Refraction data [*Gettings et al.*, 1986; *Mechie et al.*, 1986] suggest values between 8.0 and 8.15 km/s for this region. We used a version of the two-station method [e.g., *Beghoul and Barazangi*, 1989] to independently calculate the *Pn* phase velocity in the region directly under the stations as well as possible given the limited data set. Only phases with a signal-to-noise ratio > 2.0 and from events within 6°of the two-station azimuth were used. Any events with a location residual > 5 s were also eliminated. This resulted in a data set of 97 ray paths, with a mean value of 8.1 ± 0.3 km/s.

Using this value, we calculated station corrections for the stations relative to HALM (if sufficient ray paths were available). Only SODA (2.1 s) and RIYD (1.7 s) had corrections larger than the standard deviation. A recalculation of the *Pn* velocity using these corrections yielded 8.0 ± 0.2 km/s. While these results possess large standard deviations, they at least suggest that the data set is not systematically biased. We also determined the *Sn* and *Lg* velocities with the same method (Table 1). The *Sn* data (69 observations) showed considerable scatter but yielded 4.5 ± 0.5 km/s. After eliminating all data more than 1 standard deviation from the mean (resulting in 52 observations) we found 4.4 ± 0.2 km/s. *Lg* velocity was 3.6 ± 0.2 km/s, but only a small number of observations (10) were used.

The station correction for SODA is probably due to a combination of elevation (2 km higher than all other stations) and possibly anomalous crustal structure as SODA is at the edge of the Red Sea rift. RIYD lies on the sediments of the Arabian Platform. All other stations are within a few hundred meters of elevation of each other and are on Arabian Shield.

2.6. Slowness Stacks

We tested slowness stacks as a way to summarize and compare all data, as these stacks also provide a velocity estimate of the various phases. Slowness was calculated relative to the *P* arrival time, rather than the event origin time as we found that the *P* arrival times produced better results than earthquake origin times, probably due to mislocations.

The slowness stacks were created by stacking the detection stacks along lines of constant moveout. As the velocity variations for regional phases at these distances are small compared to the bin resolution, the assumption of constant moveout is reasonable. Figure 7 shows the results for the Gulf of Aqaba and the Zagros regions. The X axis is the slowness (relative to *Pn*). The Y axis is the time delay. The diagonal line marks the time delay for each slowness at a distance of 10°. The spread of energy across a wide range of slownesses (usually as linear artifacts) is due to the long duration of regional phases and poor network geometry. Only peaks on the diagonal line indicate seismic phases. The relative slowness has been converted to velocity using a *Pn* velocity of 8.1 km/s.

Again, clear differences are visible between the Gulf of Aqaba and Zagros region. The vertical component for the Gulf of Aqaba shows an increase in energy at a time of roughly 170-180 s with a reduced slowness of ~ 0.15 (3.7 km/s). This corresponds to the strong *Lg* arrival observed in Figure 4. The Zagros stack shows three distinct concentrations, due to *Pg*, *Sn*, and *Lg*, at about 0.05 (5.8 km/s), 0.09 (4.5 km/s) and 0.17 (3.5 km/s). The difference in *Lg* velocity between the Gulf of Aqaba events and the NE/Zagros events is apparent and matches the move-out on Figure 4.

3. Conclusions and Discussion

3.1. Evaluation of Stacking for Regional Waveforms

Overall, stacking of regional waveforms appears to be an effective method of quickly analyzing large amounts of data in a near automatic fashion. The stacks reflect the characteristics of the waveforms, and the relative amplitude and velocity can be measured. The advantage of the stacking is that it allows all the data to be examined simultaneously, as does a record section, but with an improved signal-to-noise ratio. While the *Pg* phase may be difficult to identify on the individual seismograms, it was easily resolved on the stacks. We also note that stacking offers the potential for accumulating statistics on the likelihood of a phase and that these

Table 1. Regional Phase Velocities as Estimated by the Two-Station Method and by Slant Stacking

Phase	Two Station	Number of Observations	Reduced Slowness	Slant Stack Velocity	Other Studies
Pn	8.0 ± 0.2	97	-	-	8.0-8.15 [1,2]
Pg	-	-	0.05	5.8	-
Sn	4.4 ± 0.2	52	0.09	4.7	-
Lg	3.6 ± 0.2	10	0.16	3.5	-

Velocity in km/s, slowness in s/km. *Pn* velocity assumed to be 8.1 km/s for *Pg*,*Sn*, and *Lg* slant stack velocities. Sources: 1, [*Mechie et al.*, 1986]; 2, [*Mooney et al.*, 1985].

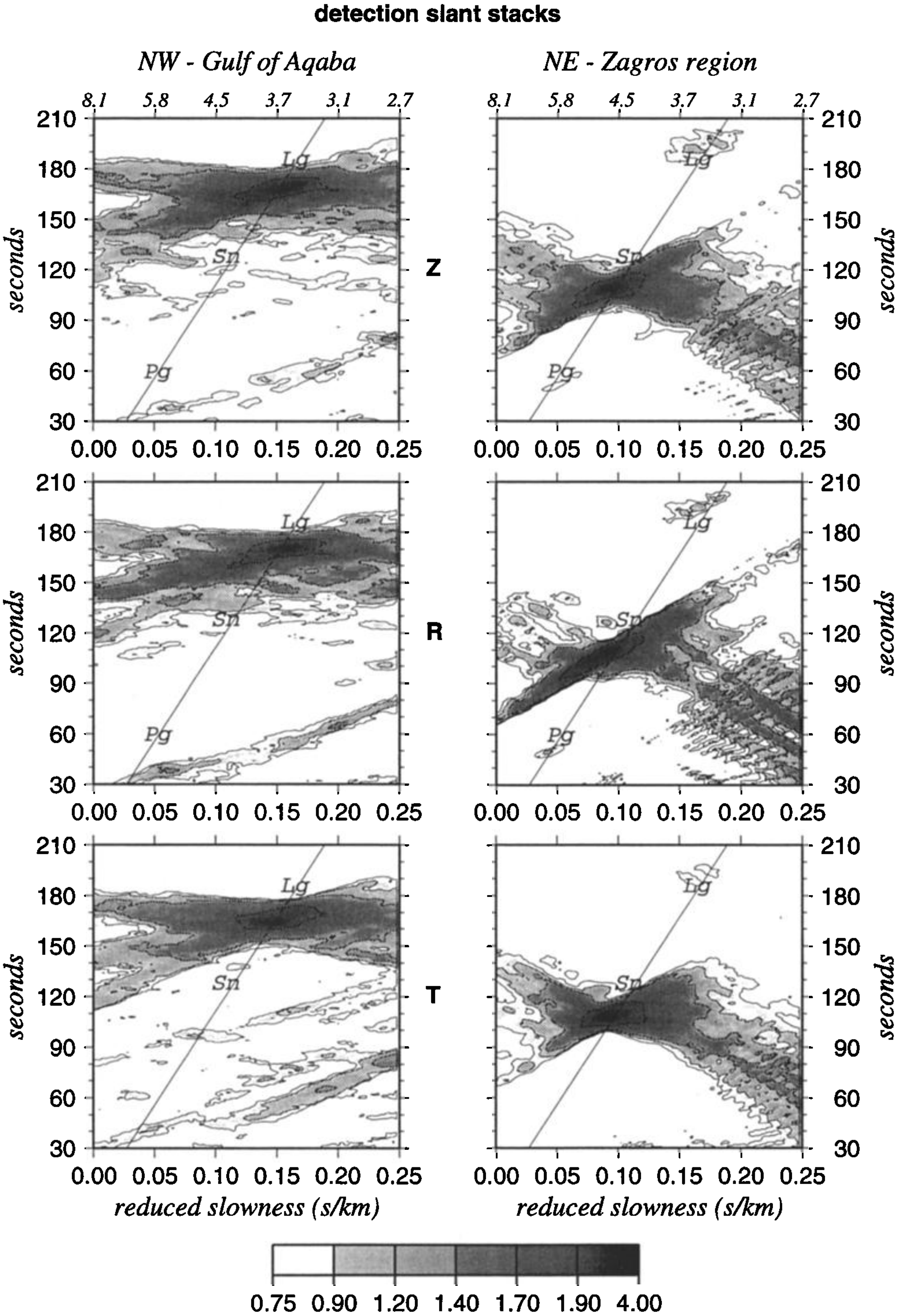

Figure 7. Slant stacks of the data from the Gulf of Aqaba and the Zagros. Both sets of stacks are normalized to each other. The contour lines represent the 70, 80, 90, and 99 percentiles. The diagonal line marks the time/slowness for a seismogram at 10°. The phase names mark the IASPEI theoretical arrival times. The velocities at the top were converted from relative slowness using a *Pn* velocity of 8.1 km/s.

statistics may be useful for both detecting and characterizing the robustness of a phase. Slowness stacks are useful for graphically comparing phase amplitude and relative velocities, but the absolute velocity accuracy was poor.

A drawback is that clusters of events must be grouped together which lowers the spatial resolution of waveform differences, especially for small data sets. Stacking does not work well for regions with extremely heterogeneous structure such as the southern Red Sea.

3.2. Tectonic Implications

We found strong variations in the regional waveforms that depended strongly on the area of origin. Events in the Zagros showed clear *Pn*, *Pg*, and *Sn* phases. The thick sedimentary basin between the Zagros and the shield appeared to have little effect on the propagation efficiency of these phases. *Lg* propagated well except from events near the Straits of Hormuz. This may be due to either thin crust in the extreme southern Arabian Gulf or topographic effects in the southern Zagros.

In contrast, events in the Gulf of Aqaba showed very weak body phases but a prominent *Lg*. It is possible that part of this may be due to source effects, as almost all of the events are aftershocks of a large strike-slip event and may have similar mechanisms. However, it is impossible for both *Pn* and *Sn* to have small amplitudes due to the focal mechanism alone. A second possibility is phase conversions at the gulf/peninsula boundary. *Sn* to *Lg* conversions often occur at continental margins [*Isacks and Stephens*, 1976; *Seber et al.*, 1993] and would explain the low *Sn* amplitude and high *Lg* amplitude.

However, phase conversions do not explain the low *Pn* amplitudes. Waveforms from events in the southern Red Sea which originate in a similar environment and also cross a continental margin show evidence of *Sn*/*Lg* conversion [*Baker et al.*, 1997] but still possess at least a weak *Pn* and *Sn* (i.e., Figure 2). Waveforms from an event east of the gulf which do not cross a continental boundary (Figure 2b) display very similar waveforms to the Gulf of Aqaba events (large *Lg* and small body phases). Therefore we believe that phase conversion effects alone cannot explain the disparity in waveforms between the Gulf of Aqaba events and from events in other directions.

We suspect that a zone of inefficient *Pn* and *Sn* propagation extends into the Arabian peninsula and well away from the Red Sea rifting. *Rodgers et al.* [1997] noted inefficient *Sn* propagation around the Gulf of Aqaba, and *Seber and Mitchell* [1992] suggested that pervasive attenuation occurs across much of the peninsula. As clear *Sn* is observed from the Zagros, the shield under the stations and to the west must allow *Sn* propagation. The large *Lg* observed at all stations for Gulf of Aqaba events indicates that crustal attenuation is low.

Inefficient *Pn* and *Sn* propagation can be caused by high attenuation in the upper mantle or possibly mantle velocity gradients that do not transmit head waves well (or a combination of both). In principle, attenuation effects should affect *S* waves more than *P* waves and will be more pronounced at high frequencies. Poor *Sn* propagation is generally attributed to a relatively hot upper mantle with a thin mantle lid. Hot upper mantle should also cause low *Pn* velocities which is not observed, suggesting that most of the stations lie at the boundary of the zone.

While regional phase blockages might be expected near the Red Sea rifting, it is surprising at first that these effects would extend well under most of the shield. However, the surface geology shows that the volcanic activity is not restricted to the rift margin. Volcanic rocks are scattered throughout, and the area has a history of active volcanism as recently as 800 years ago [*Camp et al.*, 1987]. A petrologic study of the volcanic rocks led *Camp and Roobol* [1992] to suggest that the Arabian Shield was underlain by a symmetrical, north-south zone of asthenospheric upwelling (Figure 8). The nature of the Precambrian basement appears to be a controlling factor on the distribution of this hot mantle. Accreted oceanic terranes of the western shield form the basement to numerous Cenozoic-to-Recent lava fields; the eastern shield, however, is composed of accreted continental terranes that are devoid of these Cenozoic volcanics. The denser and thinner oceanic terranes may be more susceptible to mantle upwelling and melt migration. *Camp and Roobol* [1992] suggested that the crest of upwelling occurs along the Makkah-Madinah-Nafud volcanic line, where basalt melts are derived by $\sim$ 10-15 % partial melting. Basalt lavas on the opposing sides of the volcanic line are more alkalic and derived at deeper depths and indicate smaller degrees of partial melting.

A comparison of the mantle geometry suggested by *Camp and Roobol* [1992] (Figure 8) closely matches the areas of *Pn* and *Sn* attenuation indicated in this study. All of the ray paths from the Gulf of Aqaba cross directly under the area of young volcanics. Ray paths from the event in Figure 2b are mixed as some pass under or near areas of activity, while others (e.g., to RIYD) are more removed. This indicates that the area of anomalous mantle must extend farther to the northeast than the Holocene volcanics. Ray paths from the Zagros and Arabian Sea do not pass anywhere near the volcanics and show strong *Sn*. The extensive surface volcanics as well as the xenolith data [*McGuire*, 1988] indicate that the lithosphere must be hotter than average continental shield lithosphere, a conclusion also supported by *Knox et al.* [1998]. We suspect that partial melting in the upper mantle associated with the volcanic activity and higher temperatures is responsible for the *Sn* attenuation.

An extended area of mantle upwelling away from the Red Sea has implications for mantle flow and dynamics. The overall trend of the volcanics is not parallel to the plate motion vector, and *Camp and Roobol* [1992] note

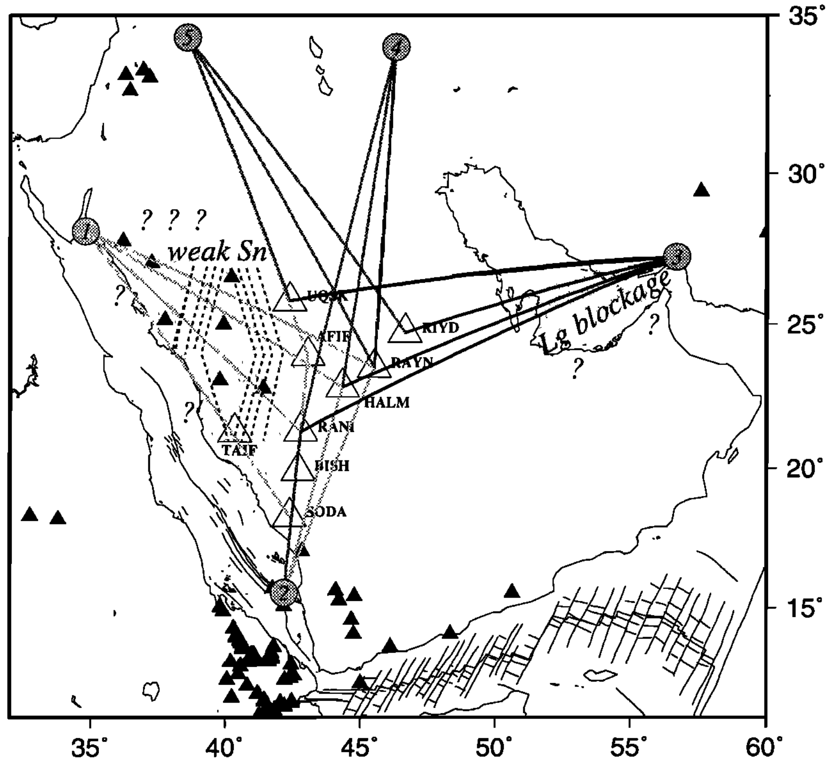

Figure 8. Map showing *Sn* ray paths from events in Figure 2 with ray path shading as in Figure 3 (solid is "efficient", shading is "inefficient", and light shading "not observed"). The stippled areas marks areas of presumed *Sn* and *Lg* blockage as mapped in this study. Question marks indicate unconstrained boundaries due to insufficient data. The dashed lines outline the area of possible asthenospheric upwelling as mapped by *Camp and Roobol* [1992] using petrologic data. Other annotations are in Figure 1. Ray paths with weak *Sn* from the Gulf of Aqaba travel almost entirely under the Holocene activity, while ray paths with strong *Sn* from the Zagros almost completely avoid it.

that eruptive activity in the individual volcanic centers shifts to the northeast over time. This behavior is not expected with a hotspot model. Shear wave splitting results [*Wolfe et al.*, 1999] indicate mantle flow is aligned roughly parallel to the plate motion. The area of suspected hot upper mantle also lies northeast of the area of active rifting in the Red Sea (as defined by magnetic lineations).

Knox et al. [1998] suggest that the high mantle temperatures may be due to small-scale convection, Red Sea rifting, or an extension of the Afar plume. Owing to the long-lived nature of the volcanic activity and the apparent mantle flow direction, the high temperatures may reflect a northward extension of the Afar plume that extends under the active rifting of southern Red Sea and then under western Saudi Arabia. *Sultan et al.*, [1993] suggested that much of the Red Sea rifting was controlled by crustal geology. Therefore it is possible that the mantle flow may not be symmetric under the axis of the Red Sea but may be shifted to the east, especially in the north. This would explain both the distribution of Holocene volcanics as noted by *Camp and Roobol* [1992] and the areas of regional phase attenuation observed in this paper.

Acknowledgments. This work was supported by an IUT grant from Lawrence Livermore National Laboratory to R. Mellors. Discussions with L. Astiz, P. Earle, D. McNamara, A. Rodgers, F. Ryall, W. Walter, and J. Zollweg greatly aided in this work. We also thank the reviewers and associate editor for useful comments.

References

Al-Amri, A. M. S., An investigation of the seismicity and the aeromagnetic features of the structural framework in the Gulf of Aqabah and the adjoining land region, Midyan, northern Red Sea, Ph.D thesis, 251 pp., Univ. of Minn.-Twin Cities, 1990.

Al-Amri, A. M. S., Seismicity of the south-western region of the Arabian Shield and southern Red Sea, *J. of Afr. Earth Sci.*, *19*, 17-25, 1994.

Al-Amri, A. M. S., Recent seismic activity in the Northern Red Sea, *J. Geodyn.*, *20*, 243-253, 1995.

Astiz, L., P. Earle, and P. Shearer, Global stacking of broadband seismograms, *Seismo. Res. Lett.*, *67*, 8-18, 1996.

Baker, G. E., T. G. Barker, and K. L. McLaughlin, Source and propagation effects on regional phase amplitudes in the Middle East (abstract), *Eos Trans. AGU, 78 (46)*, Fall Meet. Suppl., F428, 1997.

Barazangi, M., D. Seber, T. Chaimov, J. Best, R. Litak, D. Al-Saad, and T. Sarif, Tectonic evolution of the northern Arabian Plate in western Syria, in *Recent Evolution and Seismicity of the Mediterranean Region*, edited by E. Boschi, *NATO ASI Ser., Ser. C, 402*, 117-140, 1993.

Beghoul, N., and M. Barazangi, Mapping high *Pn* velocity beneath the Colorado Plateau constrains uplift models, *J. Geophys. Res.*, *94*, 7083-7104, 1989.

Camp, V. E., and M. J. Roobol, Upwelling asthenosphere beneath western Arabia and its regional implications, *J. Geophys. Res.*, *97*, 15,255-15,271, 1992.

Camp, V. C., P. R. Hooper, M. J. Roobol, and D. L. White, The Madinah eruption, Saudi Arabia: Magma mixing and simultaneous extrusion of three basaltic chemical types, *Bull. Volcanol.*, *49*, 489-508, 1987.

Camp, V. C., M. J. Roobol, and P. R. Hooper, The Arabian alkali basalt province, part II, Evolution of Harrats Khaybar, Ithnayn, and Kura, Kingdom of Saudi Arabia, *Geol. Soc. Am. Bull.*, *103*, 363-391, 1991.

Dowla, F., et al., Seismic regionalization in the Middle East and North Africa, in *Proceedings of the 18th Annual Seismic Research Symposium on Monitoring a Comprehensive Test Ban Treaty*, edited by J. F. Lewkowicz, J. M. McPhetres, and D. T. Reiter, Philips Lab., Hanscom AFB, Mass., 55-64, 1996.

Earle, P., and P. Shearer, New observations of *PKKP* precursors: Constraints on core-mantle-boundary topography at short scales, *Science*, *277*, 667-670, 1998.

Flanagan, M., and P. Shearer, Global mapping of topography on transition zone velocity discontinuities by stacking *SS* precursors, *J. Geophys. Res.*, *103*, 2673-2692, 1998.

Gettings, M. E., H. R. Blank, W. D. Mooney, and J. H. Healy, Crustal structure of southwestern Saudi Arabia, *J. Geophys. Res.*, *91*, 6491-6512, 1986.

Ghalib, H., Seismic velocity structure and attenuation of the Arabian Plate, Ph.D thesis, St. Louis Univ., St Louis, Mo., 314 pp., 1992.

Hartse, H. E., S. R. Taylor, W. S. Philips, and G. E. Randall, A preliminary study of regional seismic discrimination in central Asia with emphasis on western China, *Bull. Seismol. Soc. Am.*, *87*, 551-568, 1998.

Healy, J. H., W. D. Mooney, H. R. Blank, M. E. Gettings, W. M. Kohler, R. J. Lamson, and I. Leone, Saudi Arabian seismic deep-refraction profile, *U.S. Geol. Surv.*, Open File Rep. 83-390, 429 pp., 1982.

Hearn, T. M., and J. F. Ni, *Pn* velocities beneath continental collision zones: The Turkish-Iranian Plateau, *Geophys. J. Int.*, *117*, 273-283, 1994.

Isacks, B., and C. Stephens, Conversion of *Sn* to *Lg* at a continental margin, *Bull. Seismol. Soc. Am.*, *65*, 235-244, 1977.

Kadinsky-Cade, K., M. Barazangi, J. Oliver, and B. Isacks, Lateral variations of high-frequency seismic wave propagation at regional distances across the Turkish and Iranian Plateaus, *J. Geophys. Res.*, *86*, 9377-9396, 1981.

Kennett, B. L. N., and E. R. Engdahl, Traveltimes for global earthquake location and phase identification, *Geophys. J. Int.*, 105, 429-465, 1991.

Knox, R. P., A. A. Nyblade, and C. A. Langston, Upper mantle *S* velocities beneath Afar and western Saudi Arabia from Rayleigh wave dispersion, *Geophys. Res. Lett.*, *25*, 4233-4236, 1998.

McGuire, A. V., The mantle beneath the Red Sea margin: Xenoliths from western Saudi Arabia, *Tectonophysics*, *150*, 101-119, 1988.

McNamara, D. E., T. L. Owens and W. Walter, Observations of regional phase propagation across the Tibetan Plateau, *J. Geophys. Res.*, *100*, 22,215-22,229, 1995.

McNamara, D. E., T. J. Owens, and W. R. Walter, Propagation characteristics of *Lg* across the Tibetan Plateau, *Bull. Seismol. Soc. Am.*, *86*, 457-469, 1996a.

McNamara, D., W. Walter, C. Schultz, and P. Goldstein, Regional phase propagation in northern Africa and the Mediterranean (abstract), *Seismol. Res. Lett.*, *67*, 47, 1996b.

Mechie, J., C. Prodehl, and G. Koptschalitsch, Ray path interpretation of the crustal structure beneath Saudi Arabia, *Tectonophysics*, *131*, 333-352, 1986.

Mellors, R., Preliminary noise survey and data report of Saudi Arabian data, *UCRL-ID-128949*, 15 p, Lawrence Livermore Nat. Lab., Livermore, Calif., 1997.

Mitchell, B. J., and Y. Pan, *Lg* coda variation across Eurasia and its relation to continental evolution (abstract), *Eos Trans. AGU, 77 (46)*, Fall Meet. Supple., F474, 1996.

Molnar, P., and J. Oliver, Lateral variations of attenuation in the upper mantle and discontinuities in the lithosphere, *J. Geophys. Res.*, *74*, 2648-2682, 1969.

Mooney, W. D., M. E. Gettings, H. R. Blank, and J. H. Healy, Saudi-Arabian seismic-refraction profile: A traveltime interpretation of crustal and upper mantle structure, *Tectonophysics*, *111*, 173-246, 1985.

Richards-Dinger, K. and P. Shearer, Estimating crustal thickness in southern California by stacking *PmP* arrivals, *J. Geophys. Res.*, *102*, 15,211-15,242, 1997.

Rodgers, A. J., J. F. Ni, and T. M. Hearn, Propagation characteristics of short-period *Sn* and *Lg* in the Middle East, *Bull. Seismol. Soc. Am.*, *87*, 396-413, 1997.

Ross, D., E. Uchupi, and R. S. White, The geology of the Persian Gulf-Gulf of Oman region: A synthesis, *Rev. Geophys.*, *24*, 537-556, 1986.

Sandvol, E., D. Seber, M. Barazangi, F. Vernon, R. Mellors, and A. Al-Amri, Lithospheric seismic velocity discontinuities beneath the Arabian Shield, *Geophys. Res. Lett.*, *25*, 2873-2876, 1998.

Seber, D., M. Vallve, E. Sandvol, D. Steer, and M. Barazangi, Middle East Tectonics: Applications of Geographic Information Systems (GIS), *GSA Today*, *7*, 1-6, 1997.

Seber, D., and B. J. Mitchell, Attenuation of surface waves across the Arabian Peninsula, *Tectonophysics*, *204*, 137-150, 1992.

Seber, D., M. Barazangi, B. A. Tadili, M. Ramdani, A. Ibenbrahim, D. B. Sari, and S. O. El Alami, *Sn* to *Sg* conversion and focusing along the Atlantic margin, Morocco: implications for earthquake hazard evaluation, *Geophys. Res. Lett.*, *20*, 1503-1506, 1993.

Shearer, P., Imaging global body wave phases by stacking long-period seismograms, *J. Geophys. Res.*, *96*, 20,353-20,364, 1991.

Shearer, P., Imaging Earth's seismic response at long periods, *Eos Trans. AGU*, *75*, 449,451-452, 1994.

Stoeser, D. B., and V.E. Camp, Pan-African microplate accretion of the Arabian Shield, *Geol. Soc. Am. Bull.*, *96*, 817-826, 1985.

Sultan, M., R. Becker, R. E. Arvidson, P. Shore, R. J. Stern, Z. El Alfy, and R. I. Attia, New constraints on Red Sea rifting from correlations of Arabian and Nubian neoproterozoic outcrops, *Tectonics*, *12*, 1303-1319, 1993.

Vernon, F. L., R. J. Mellors, J. Berger, A. M. Al-Amri, and J. Zollweg, Initial results from the deployment of broadband seismometers in the Saudi Arabian shield, in *Proceedings of the 18th Annual Seismic Research Symposium on Monitoring a Comprehensive Test Ban Treaty*, edited by J. F. Lewkowicz, J. M. MacPhetres, and D. T. Reiter, Philips Lab., Hanscom AFB, Mass., 108-117, 1996.

Vidale, J. E., and H. M. Benz, High-resolution sounding of upper mantle discontinuities (abstract), *Eos Trans. AGU, 73 (43), Fall Meet. Suppl.*, 518, 1992.

Walck, M. C., and R. Clayton, Analysis of upper-mantle structure using wave-field continuation of *P*-waves, *Bull. Seismol. Soc. Am.*, *74*, 703-719, 1984.

Wessel, P., and W. H. F. Smith, New version of the Generic Mapping Tools released, *Eos Trans. AGU*, *76*, 329, 1995.

Wolfe, C. J., F. L. Vernon, and A. Al-Amri, Shear-wave splitting across western Saudi Arabia: The pattern of upper mantle anistropy at a Proterozoic shield, *Geophys. Res. Lett.*, *26*, 779-782, 1999.

A. M. S. Al-Amri and A. Ghalib, Department of Geology, King Saud University, Riyadh, Kingdom of Saudi Arabia

V. E. Camp and R. J. Mellors, Department of Geological Sciences, San Diego State University, San Diego CA 92182. (rmellors@geology.sdsu.edu)

F. L. Vernon, Cecil and Ida Green Institute of Geophysics and Planetary Physics, Scripps Institute of Oceanography, La Jolla, CA 92093. (flvernon@ucsd.edu)

(Received August 28, 1998; revised March 26, 1999; accepted May 25, 1999.)